

TRAJECTORY AND NAVIGATION DESIGN FOR AN IMPACTOR MISSION CONCEPT

Andres Dono Perez^{*}, Roland Burton[†], Jan Stupl[‡], and David Mauro[§]

This paper introduces a trajectory design for a secondary spacecraft concept to augment the science return in interplanetary missions. The concept consists of a single-string probe with a kinetic impactor on board that generates an artificial plume to perform in-situ sampling. A Monte Carlo simulation was used to validate the nominal trajectory design for a particular case study that samples ejecta particles from the Jupiter's moon Europa. Details regarding the navigation, targeting, and disposal challenges related to this concept are presented herein.

INTRODUCTION

The design of multiple trajectories for secondary spacecraft enables the application of novel concepts to extend the science return of interplanetary missions. Small spacecraft are attractive from a cost perspective, and they are able to accept higher risks. A single-string approach fits the development of secondary mission concepts, since the requirements in lifetime, operations, and redundant systems are less stringent.

This paper describes the trajectory design and validation method for a single-string mission concept that allows the analysis of sub-surface samples without landing. In this concept, a probe is attached as a secondary payload to a larger interplanetary spacecraft. This probe carries an inert impactor that is deployed to produce a hypervelocity collision with a target celestial body. This event creates an ejecta cloud that allows the mother probe to pass through the expelled particles and gather samples subsequently. The trajectory design is applied to a particular case study of this concept in the vicinity of Jupiter's moon Europa.

We start with an overview of secondary missions and their potential in the application of innovative concepts. This section also includes an introduction to the case study and the high level constraints that define the trajectory design trade space. A nominal solution is found posteriorly that complies with the requirements imposed by those constraints. Details about the used trajectory validation method as well as the considered assumptions are also included. The results of the validation technique present the data obtained in the analysis and an include an interpretation to address mission performance. An estimated propulsion budget for the trajectory corrections is available in this data set. The last sections introduce some recommendations for future work and a brief analysis of two heritage mission examples where the trajectory design could have been applied.

^{*}Trajectory Analyst, Millennium Engineering and Integration Services, NASA Ames Research Center, Moffett Field, CA, USA

[†]Consultant, Millennium Engineering and Integration Services, NASA Ames Research Center, Moffett Field, CA, USA

[‡]Research scientist, Stinger Ghaffarian Technologies Inc., NASA Ames Research Center, Moffett Field, CA, USA

[§]Systems Engineer, Stinger Ghaffarian Technologies Inc., NASA Ames Research Center, Moffett Field, CA, USA

BACKGROUND

Secondary spacecraft

Secondary payloads, or rideshares, are small payloads included on a launch vehicle along with a main spacecraft, exploiting the extra volume that is not utilized by the primary. The fundamental benefit of these payloads is the reduced cost for transportation. The downsides include the absence of control to choose the launch date and the target orbit parameters, and the lack of flexibility in the integration with the primary.

Interplanetary missions provide a substantial opportunity for secondary spacecraft since the orbit transfer can be performed either by the upper stage of the launch vehicle, or by the primary. As a consequence, small spacecraft are able to leave the Earth sphere of influence at no transfer propellant expense. At the destination, the inexpensive spacecraft can offer innovative concepts of operations.

An example of an interplanetary mission is the Europa Multiple Flyby Mission (EMFM), that plans to insert a spacecraft to the Jovian system to perform several flybys of Europa and other Galilean moons. The mission objectives are to assess the habitability of Europa by studying its ice shell, composition, and geology. Recent observations with the Hubble Space Telescope have shown the existence of natural water vapor plumes in Europa that expelled sub-surface material to high altitudes.⁹ Knowledge about the composition of the particles of the plume is very valuable. The plumes are believed to expel water from a theoretical subsurface ocean in Europa.⁹ The extremely tenuous atmosphere of Europa would enable a spacecraft to obtain samples by performing a flyby at a low altitude through the resulting ejecta cloud. Hence, data from underneath the surface of the moon can be obtained without the complexity of a lander mission.

EMFM is susceptible to encounter a plume while performing one of its Europa flybys. However, to gather relevant data, the spacecraft needs to pass through a high concentration of the expelled material and that imposes a significant risk to the mission. In addition, EMFM needs to alter its trajectory if the plume appears in another location other than the planned flyby approach. To overcome this issue, a secondary spacecraft is able to accept higher risks and to modify its own trajectory to target a fitting B-plane aim point to obtain data from a potential plume event. However, there are two main challenges. The first one is that the plume would need to be on the limb of Europa to allow the spacecraft to avoid an impact with the moon. The second is that the plume has to manifest while the spacecraft is in close proximity to the body. The likelihood of a natural occurrence is not consistent, since plume activity in Europa is believed to be variable.⁹

The non existence of a natural plume is a major risk that can be avoided by creating an artificial plume. A secondary spacecraft mission can perform a hypervelocity impact through the release of a Kinetic Impactor (KI). This provides a competitive advantage, since the plume can be created at any desired point in time. The Europa Life Signature Assayer (ELSA) mission concept consists of a probe that is flown as a secondary payload with the EMFM. ELSA would use its own KI to excavate sub-surface particles and catapult them to altitudes where it would be able to pass through to collect samples.

The trajectory design presented here is the result of an analysis to develop the ELSA mission concept. The concept originated as part of a study at the Mission Design Division, at the NASA Ames Research Center. The outcome of this effort conceived the utilization of a small spacecraft as a secondary payload to Europa to augment the science return of the EMFM.

High level constraints

The following high level constraints materialize due to the fact that the investigated ELSA concept is a secondary mission in the Jovian system. These constraints bound the available trade space for the trajectory design.

- No modification and interference with respect to EMFM trajectory.
- Science return: the secondary spacecraft has to create an artificial impact with a KI and gather samples from the plume by flying through it, and without impacting Europa.
- Planetary Protection requirements: the secondary spacecraft must not impact Europa at any point in time.
- An available and maximum mass budget of 250 kg, including margins.

TRAJECTORY DESIGN

Implication of constraints.

The high level constraints have severe implications in the mission trade space that define the requirements of the trajectory design.

No interference. Following release, ELSA must wait to start operations until there is no risk to interfere with EMFM.

Science. The Planetary Systems Branch at NASA Ames Research Center conducted an analysis to study the outcome of the hypervelocity impact. A plume model based on Europa impacts was applied to study the effects of various impact configurations. An impact with a target flight path angle (FPA) of 15 deg, gives a requirement of passing the resulting plume at altitudes between 50-100 km to gather significant data. The maximum particle concentration occurs 120 seconds after the impact, and the resulting cloud width is 94 km. The analysis also concluded that a simultaneous measurement of both primary and secondary spacecraft, at different flyby altitudes, would add greater value to the obtained data. Therefore, ELSA needs to match the B-plane parameters of the EMFM flyby and time the release of the impactor in a way that both spacecraft pass through the plume 120 seconds after the collision.

Planetary protection. Regulations state that the spacecraft must not impact Europa since it carries hazardous components such as propellant or batteries that may contaminate this potentially habitable world. Therefore, ELSA must avoid Europa in its close encounter and it needs to perform a disposal strategy that eliminates any risk of impacting any protected object after the mission is decommissioned. To comply with the avoidance requirement while maximizing science return, initial analysis showed that the KI has to impact at a FPA of 15 deg to allow the probe to pass through the cloud and still avoid an impact with Europa at periapsis. The KI must not have any electronic or hazardous elements and has to be exposed to high temperatures before integration into the spacecraft to eliminate any microorganism that could compromise the potential forms of life existent in Europa.

Spacecraft size. The size of the spacecraft has a strong influence in the trajectory trade space since it implies a limitation in the propellant mass. The spacecraft needs to be sufficiently light weight to comply with the total mass limit while still carrying the KI, the necessary subsystems,

and the scientific instruments to perform the mission. The size also has implications in the power subsystem of the spacecraft. Solar panels are heavy and not efficient for applications at far distances from the Sun. Therefore, the spacecraft is powered by batteries that also limit the lifetime of the mission. Planetary protection considerations tie with this consideration since a limit in the spacecraft lifetime implies the necessity of a rapid disposal. Since there is a restriction in the propellant mass budget, the disposal needs to be addressed via a direct impact with another moon in the Jovian system.

Flyby survey

This paper uses the 13F7-A21 ephemeris version to model the EMFM trajectory.⁴ EMFM performs a total of 45 flybys at Europa with different approaches in an effort to achieve a wide coverage of the moon. EMFM trajectory targets a launch in 2021, with a Jupiter Orbital Insertion (JOI) maneuver in 2028.⁴ The flyby schedule of the 13F7-A21 ephemeris was used to find flyby opportunities in the main mission that satisfy the implications of the high level constraints for the trajectory design of the secondary spacecraft. The survey consisted of the study of each individual flyby to calculate the ΔV associated with the deployment of the impactor, posterior Europa avoidance, and final rapid disposal.

The post-flyby conditions of the probe are paramount to fulfill planetary protection requirements. The effects caused by a gravity assist of each flyby hyperbolic approach with respect to Europa determine the trade space. If the flyby of the parent spacecraft already provides a subsequent encounter with another body, the secondary spacecraft can take advantage from targeting a similar B-plane at a lower altitude. However, depending on the specific case, a modification of the target B-plane can act in favor to uncover other opportunities that were not identified at a first sight in the primary spacecraft flyby schedule.

The resulting hyperbolic excess velocity magnitude, v_∞ , of a gravity assist is conserved between the incoming and the outgoing asymptotes with respect to the target celestial body. There is a rotation in the v_∞ vector that implies an applied change in velocity, or ΔV . The parameter that determines this rotation is known as the bending angle, which is represented in Equation 1. The resulting ΔV can also be calculated and is shown in Equation 2.⁵

$$\sin \frac{\theta}{2} = \frac{\mu}{\mu + r_p \cdot v_\infty^2} \quad (1)$$

$$\Delta V = \frac{2 \cdot v_\infty \cdot \mu}{\mu + r_p \cdot v_\infty^2} \quad (2)$$

, where θ is the bending angle, μ is the gravitational parameter of the flyby body, v_∞ is the hyperbolic excess velocity, and r_p is the periapsis radius of the hyperbola. The results of the post-flyby study have to optimize a succeeding and inexpensive disposal in terms of propellant mass.

Each of the Europa flyby opportunities existing in the EMFM 13F7-A21 trajectory were analyzed to address the feasibility of a rapid disposal at a low ΔV expense. The survey included an assessment of the ΔV required to perform the impact maneuver to release the KI and the avoidance maneuver for the probe. Out of the 45 Europa flybys that EMFM performs, 41 comply with the ΔV budget available to perform these two phases of the trajectory. However, we also needed to guarantee an immediate disposal by impacting in either Ganymede, Io, Jupiter or Callisto, while complying with our mass constraints. Hence, the focus was initially placed on finding a suitable geometry that would

lead to an immediate disposal in one of these bodies. Of the 41 remaining flybys, only one satisfied the requirements of the secondary spacecraft mission. The most suitable segment was found in a pi-transfer between Europa and Callisto within less than six days.

The existence of a pi-transfer between two bodies provided an advantageous disposal opportunity. Pi-transfers are often included in the satellite tours of interplanetary mission. They represent a non-resonant type, where the time of flight does not correspond to an integer multiple of the target body orbit.¹⁰ Pi-transfers are time efficient and allow the main spacecraft to perform consecutive approaches to a body at opposites orbital positions. For the case of 13F7-A21 EMFM ephemeris, this corresponds to Europa flyby number 28, followed by Callisto flyby number 3.⁴

There are other EMFM trajectory designs that included different gravity assists and arrival dates. These other proposed EMFM flyby tour designs also included at least one pi-transfer to change the orientation of their flyby approach.¹ However, the analysis of these alternatives is out of the scope of this paper.

Nominal design

The following describes a nominal trajectory design that starts before Europa flyby number 28 of the 13F7-A21 EMFM ephemeris. The concept of operations is defined by four critical events and starts with the release of ELSA from EMFM. The probe is released twelve hours before the main spacecraft achieves its closest approach with respect to Europa, in order to allocate time for a checkout period. After being deployed, ELSA performs a maneuver that places it in a impact trajectory with Europa to release the KI. Right after that, the probe performs an avoidance maneuver that places it in a trajectory that passes right above the impact location to gather samples. This trajectory matches EMFM B_θ targeting at a lower altitude. The epoch of this maneuver is important since it has implications on the size of the spacecraft due to a compromise between propellant mass and precision. An earlier maneuver usually requires lower ΔV but it may require more corrections if perturbations are taken into account. Finally, a disposal maneuver is performed to ensure a controlled collision with Callisto to satisfy planetary protection regulations. This last maneuver is commanded after the science data is processed and sent back to EMFM.

The mission assumes the utilization of optical and terrain relative navigation (TRN). The ELSA spacecraft relies on autonomous navigation software for trajectory determination, image processing and maneuver execution. This software has been widely used in previous interplanetary missions, such as Stardust or EPOXI, with highly accurate and successful performance.⁸ Figure 1 shows a representation of the flyby geometry at the time of close approach with Europa, as well as images of the impact and avoidance trajectories, and the disposal scenario at Callisto.

The following subsections include a more detailed explanation of each of the four critical events.

Release. At T-12 hours, where T is defined as the time of impact, ELSA and the impactor, which is carried inside, are released from EMFM. A deployment vector in the velocity direction was selected to maximize immediate separation and therefore minimizing the risk of recontact between the primary and the secondary spacecraft. The probe needs to be powered as soon as it is released. Therefore, the epoch of this event has to be selected carefully to minimize allocated mass for the batteries, and to enable the probe to separate from the primary in time before the first maneuver takes place.

Impact. At T-6 hours, the spacecraft performs a maneuver to enter a trajectory that will impact Europa. The requirements are a Flight Path Angle (FPA) of 15 degrees and a B_θ angle of

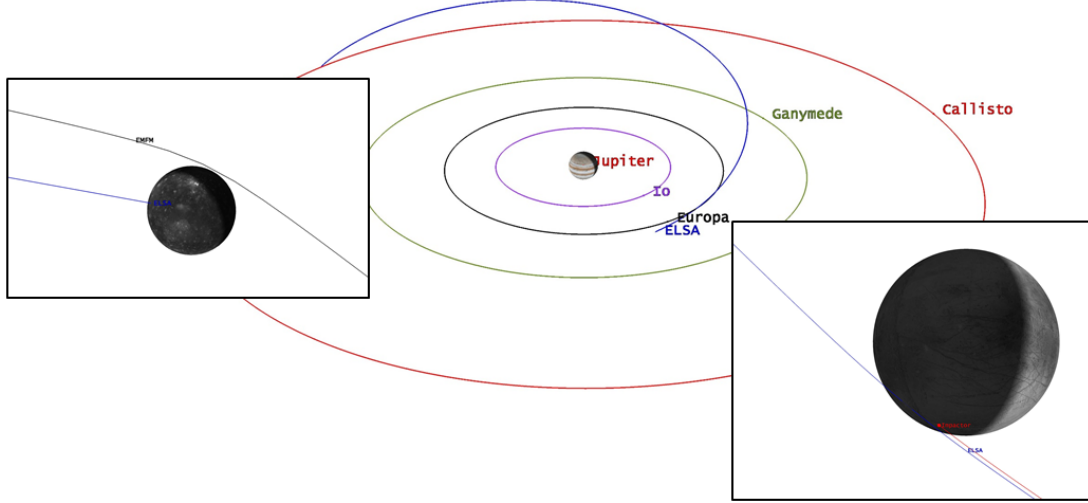


Figure 1. View of the nominal trajectory. Right image: the secondary spacecraft (shown in blue) performs a flyby through the ejecta cloud that was previously generated by the kinetic impactor (shown in red). Left image: the secondary spacecraft (shown in blue) impacts Callisto, while EMFM (shown in black) is in direct line of sight.

109.5 degrees at the time of impact, in order to follow the same trajectory as EMFM and to comply with science requirements. The maneuver is calculated to ensure that both ELSA and EMFM pass through the ejecta cloud at exactly 120 seconds after impact to target maximum particle concentration.

Avoidance. This is the most critical phase of the mission since this maneuver places the probe in a trajectory to gather the science data and avoid impacting Europa. The target flyby altitude at periapsis is set to 15 km. This gives the spacecraft a sufficiently low altitude when flying through the ejecta cloud of 75 km for the nominal case. The avoidance maneuver occurs at T-4 hours.

Disposal. The last phase consists of a maneuver that places the spacecraft in a direct impact trajectory with Callisto. To maximize execution success, the maneuver targets the center of the moon. The impact occurs 5 days after the mission is performed. This allows the spacecraft to comply with power requirements by staying alive with the on board batteries through the whole lifetime. The nominal maneuver happens at T+12 hours to allow sufficient time to process the data and relay it back to EMFM.

Trajectory Validation

The nominal trajectory was validated with a Monte Carlo simulation that considered the navigation performance of the mission. The nominal trajectory corresponds to a point design that satisfies the requirements. However, inaccuracies in the orbital determination and maneuver performance introduce deviations from the nominal result.

The simulation applies errors in the execution and knowledge of the state of the spacecraft during each of the critical events in order to calculate the Trajectory Correction Maneuvers (TCM) that are needed to guarantee mission feasibility. Figure 2 shows a sketch that presents a brief explanation of the Monte Carlo method.

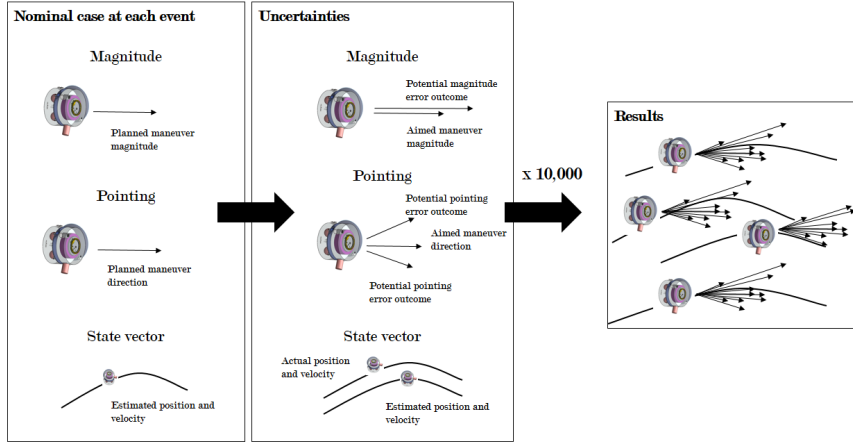


Figure 2. Representative diagram of the Monte Carlo method. The position and velocity of the spacecraft is modified to model the navigation uncertainties. An estimated state vector is implemented at each critical maneuver to calculate the direction and magnitude of the required TCMs to fulfill the mission. Each maneuver has also an execution error that is modeled by taking the propulsion system performance of the spacecraft into account.

A software framework was built to compute the statistical distributions required to model the perturbations. The initial unaltered state vectors at each critical epoch are obtained from the result of the propagation of the nominal case. These data are transferred to the software to introduce errors modeled with Gaussian distributions that perturb the state vector and address the navigation inaccuracies. Hence, an updated vector with the implemented errors is created at each critical epoch that corresponds to an estimated position and velocity state. This new configuration is propagated to compute the magnitude and direction of the TCMs that target the required parameters at each step.

Assumed orbital determination errors were based on the performance of AutoNav and TRN in previous missions. While this estimation attempts to represent an educated assumption of the current optical navigation capabilities, it is not the scope of this paper to replicate the exact data from any particular flown or planned spacecraft system. The aim is to present results that correspond with a set of assumptions to demonstrate the ability to address the navigational challenges with a statistical analysis.

This paper considers two set of assumptions to evaluate the applicability of the trajectory design in an enclosed navigation performance trade space. The first set, case I, corresponds to a scenario where there is no update in the state of the spacecraft at any point of time and that all axes have the same error. The second set, case II, assumes that there is a principal axis with more uncertainties and that the state vector knowledge is updated as the spacecraft approaches its close approach with Europa. This case also implemented changes to see how that would improve the statistical results. The epoch of the impact into Callisto was targeted to match the close approach of EMFM with this moon, this resulted in a slightly higher ΔV for the disposal maneuver. Figure 1 previously showed a representation of that nominal trajectory where both spacecraft are in view at that instant. This simulation also included the application of an added TCM to attempt an improvement in the accuracy of the spread of the impact location. Table 1 and Table 2 shows the position and velocity assumptions at each epoch for each of these approaches.

Table 1. Case I state vector uncertainty assumptions at each critical event.

Event	X (km)	Y (km)	Z (km)	Vx (m/s)	Vy (m/s)	Vz (m/s)
All events (1- σ)	1	1	1	1	1	1

Table 2. Case II state vector uncertainty assumptions at each critical event. The magnitude uncertainties decreases as the spacecraft gets closer to Europa. Navigation performance is assumed to improve when the spacecraft gets closer to the body.

Event	X (km)	Y (km)	Z (km)	Vx (cm/s)	Vy (cm/s)	Vz (cm/s)
Impact maneuver (1- σ)	10	1	1	10	5	5
Impact TCM (1- σ)	1	0.5	0.5	5	1	1
Avoidance maneuver (1- σ)	1	0.5	0.5	5	1	1
Avoidance TCM(1- σ)	0.5	0.05	0.05	1	0.5	0.5
Disposal maneuver (1- σ)	30	5	5	30	10	10
Disposal TCM1 (1- σ)	20	2	2	20	7	7
Disposal TCM2 (1- σ)	10	1	1	10	5	5

The software models the maneuver execution errors that pertain to the propulsion and ADCS systems of the spacecraft. Both inaccuracies in magnitude and pointing are introduced. The process starts with computing a maneuver to achieve the target parameters, each time the state vector uncertainties are included. Once this targeter has converged, the magnitude errors take place by altering the norm of the maneuver vector. After that, pointing errors are included by applying a rotation around the unit vector of the original maneuver. The angle of rotation is determined by the selected statistical distribution. Equation 3 shows the applied rotation matrix,⁷ where \mathbf{u} represents the unit vector of the original maneuver, i.e, the axis used for the rotation, \otimes is the tensor product, \mathbf{I} is the identity matrix, \mathbf{u}_\times is the cross product matrix of the unit vector, and ϕ is the angle of rotation.

$$\mathbf{R} = \cos \phi \mathbf{I} + \sin \phi [\mathbf{u}]_\times + (1 - \cos \phi) \mathbf{u} \otimes \mathbf{u} \quad (3)$$

The process is applied for each critical event, after introducing state vector errors at each iteration of the Monte Carlo simulation. Once all the uncertainties are included, the simulation propagates the trajectory to obtain the final outcome. The analysis of the Monte Carlo results set the magnitude and direction of the planned TCMs that are shown in Table 4. This analysis consisted of a total of 10,000 simulations to generate a ΔV budget for the TCMs to perform the mission with a high level of confidence.

Table 3. Propulsion execution error assumptions that were applied in the Monte Carlo simulation. Both pointing and magnitude errors were considered for each of the critical maneuvers as well as the TCMs. Values correspond to RCS thrusters in the EMFM.³

Uncertainties	Proportional	Fixed (mm/ s)
Magnitude (1- σ)	1%	1.17
Pointing (1- σ)	6.0×10^{-3} rad per axis	1.33 per axis

A log-normal distribution is used to model the release ΔV of the ELSA spacecraft from EMFM. The parameters are a mean of 1 m s^{-1} and a standard deviation of 10%. All values are therefore positive, in concordance with the assumption of ELSA being deployed from EMFM in the velocity direction. Range data between ELSA and EMFM was collected for each iteration of the Monte Carlo simulation to study a potential recontact between the two spacecraft.

Previous work from the EMFM maneuver execution error model included in Martin-Mur et al., 2014 and Valerino et al., 2014^{2,3} was leveraged to implement the propulsion system performance assumptions. These publications addressed the maneuver execution errors that they expect from the on board thrusters. EMFM carries two different propulsion systems, a bi-propellant engine assembly is utilized for main and large maneuvers while a reaction control system (RCS) is used for smaller maneuvers. Since our probe has a mass that is an order of magnitude smaller than EMFM, we assume the same errors than for the RCS reference. Table 3 shows the assumed performance uncertainties of the on board propulsion system for each of the maneuvers.³

RESULTS

The Monte Carlo analysis was performed by running a total of 10,000 cases for each of the two set of assumptions. The resulting data was stored and processed to produce a set of graphs that represent the statistical spread from the nominal case. Figure 3 shows a summary chart of each of the different phases of the mission as well as a timeline of the TCMs included in the final ΔV budget. Table 4 complements the chart with information about the requirements at each phase.

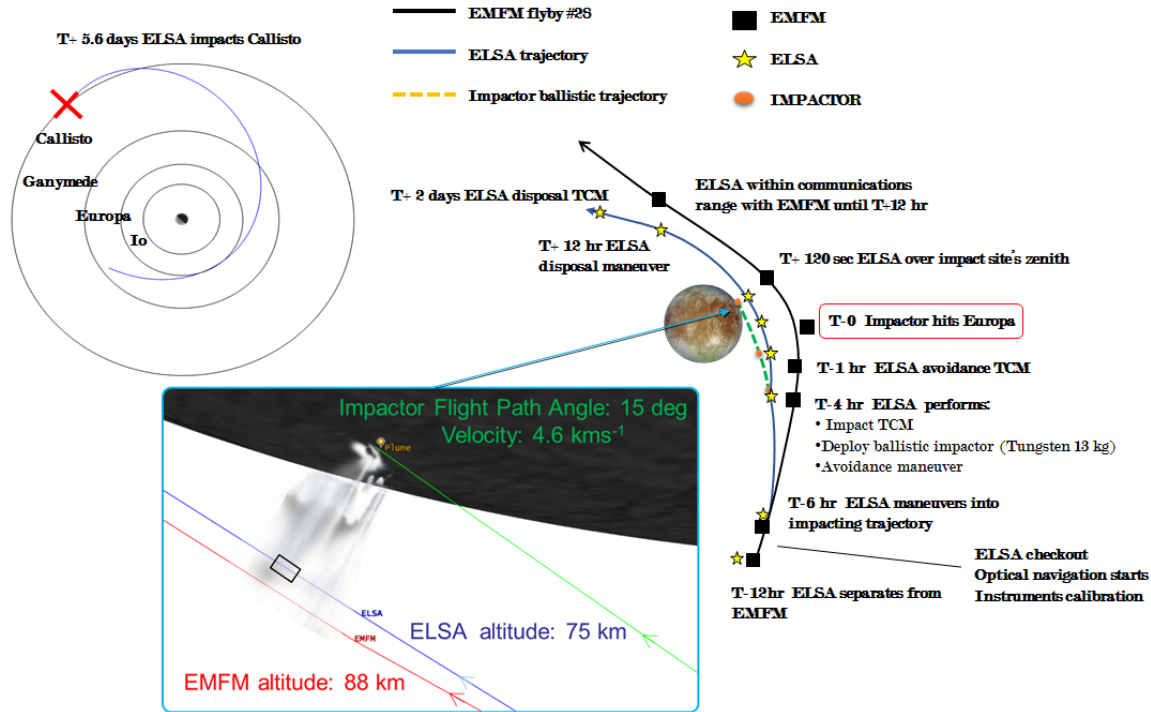


Figure 3. ELSA concept of operations and timeline of events. ELSA needs to separate 12 hours before the flyby to allow time to perform the impact and avoidance maneuvers. The disposal occurs 5.6 days after the data is gathered, ending the mission.

Table 4. Critical phase breakdown table. Each maneuver has a defined set of requirements. TCMs are included.

Phase	Target parameters	Timing	Requirements
Deployment	Sufficient range with EMFM after running all uncertainties	T-12 hr.	Separation occurs in the velocity vector.
Impactor	B_θ = same than EMFM. Collision trajectory with Europa. Impact occurs exactly 2 min before EMFM flies over the ejecta cloud.	T-6 hr for nominal. T-4 hr for TCM.	Impact success rate of 100% after statistical analysis. Same B_θ than EMFM.
Avoidance	B_θ = same than EMFM. Flying through ejecta occurs exactly at T+2 min and at the same time than EMFM.	T-4 hr for nominal. T-1 hr for TCM.	Avoidance success rate of 100% after statistical analysis. Suitable post-flyby conditions to ensure disposal. Sufficient range with EMFM to avoid any re-contact.
Disposal	Target Callisto center.	T+12 hr for nominal. T+2.5 days for TCM.	First maneuver needs to be performed at least at T+6 hr to allow time to process and relay data

Table 5. ΔV results of the Monte Carlo analysis for Case I. This table quantifies the ΔV mean magnitude as well as the standard deviation after considering a total of 10,000 simulations.

	Impact (m/s)	TCM 1 (m/s)	Avoidance (m/s)	TCM 2 (m/s)	Disposal (m/s)	TCM 3 (m/s)
Mean	23.36	2.43	36.99	6.64	21.81	3.76
σ	0.28	1.02	1.09	2.81	6.48	5.71

Data analysis produced statistics about the outcome of the Monte Carlo simulation. Table 5 Table and 6 list each maneuver's ΔV with its associated mean and standard deviation for each assumption approach. Each simulation computed results related to the performance of each of the critical phases such as the resultant B_θ angle, FPA, primary-secondary range, and altitude.

Table 5 shows the results of the Monte Carlo simulation for the first case. The standard deviation grows in the last phases of the trajectory, being the highest in the last TCM. This can be explained due to the higher separation in time between this maneuver and all the rest. The effects of the uncertainties from the previous maneuver execution is accumulated since there are not corrections for the propagation in a long time frame.

The application of the second set of assumptions resulted in a distribution with a smaller standard deviation for each of the maneuvers. Table 6 shows the resulting ΔV data. The results were significantly improved in these terms for the last TCM. The higher ΔV in the disposal maneuver with respect to Case I is due to the epoch targeting to match the EMFM flyby schedule at Callisto.

Table 6. ΔV results of the Monte Carlo analysis for Case II. This table quantifies the ΔV mean magnitude as well as the standard deviation after considering a total of 10,000 simulations.

	Impact (m/s)	TCM 1 (m/s)	Avoidance (m/s)	TCM 2 (m/s)	Disposal (m/s)	TCM 3 (m/s)	TCM 4 (m/s)
Mean	26.18	0.72	36.97	1.48	35.22	2.04	1.13
σ	0.30	0.42	0.37	0.85	1.99	1.43	0.62

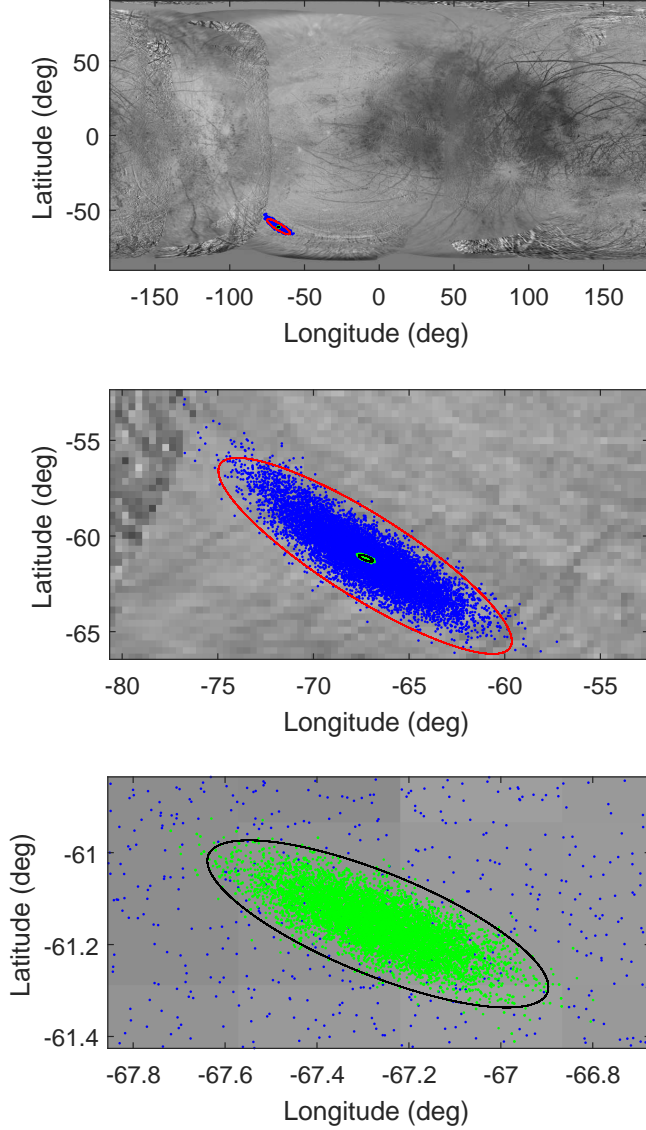


Figure 4. Location of the impact that correspond each of the ten thousand iterations for the two set of assumptions. Each blue dot is associated with an iteration of the analysis for Case I. The smaller ellipse in the third figure with the green dots represents the results of Case II.

Figure 4 shows three plots that show the end product of the entire Monte Carlo simulation for each the two cases. The blue dots correspond to the first approach, while the green dots are the result of the second approach. The 3σ ellipse is drawn in red and black respectively. The consequence of an improved set of assumptions are discernible in the third plot that is encapsulated in a small region close to the target location of the nominal trajectory.

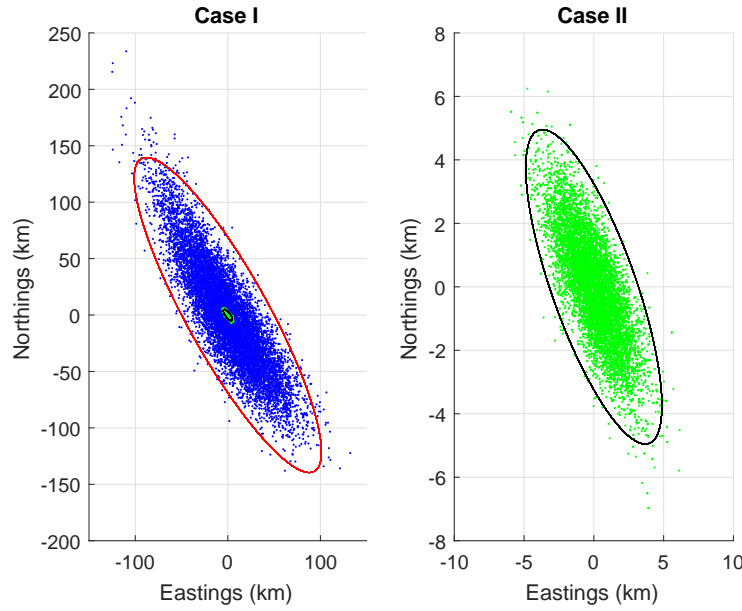


Figure 5. Close-up view of the results of the Monte Carlo simulations with information about the distances in km from the nominal case. The first and second plots correspond to the conservative and optimistic set of assumptions respectively.

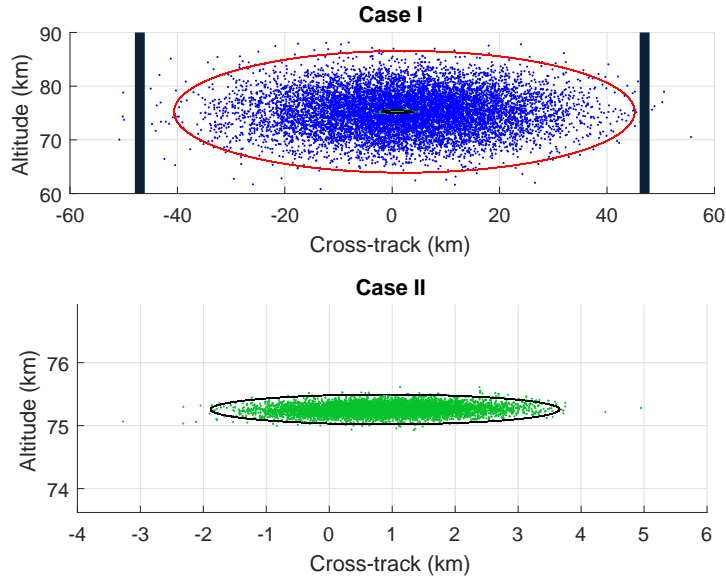


Figure 6. 3- σ ellipse of flight path variation through the ejecta cloud. The two vertical lines represent the expected plume width. Ten thousand cases are illustrated for each case. Blue dots represent the results from Case I while the green dots are the results of Case II.

Figure 5 shows two other views that represent the distance in kilometers from the nominal impact location for each of the cases separately. The first picture corresponds to Case I simulation while the second represents Case II. The results show that there is a difference by an order of magnitude in the distance of the 3σ ellipse for the nominal case.

Figure 6 shows the consequence of the avoidance event. Here, the vertical lines represent the expected ejecta cloud diameter. For Case I, a small percentage of the points are outside the expected plume width. In contrast, all points are inside the boundaries by a large margin for Case II. These events correspond to the time of maximum particle concentration, 120 seconds after the impact.

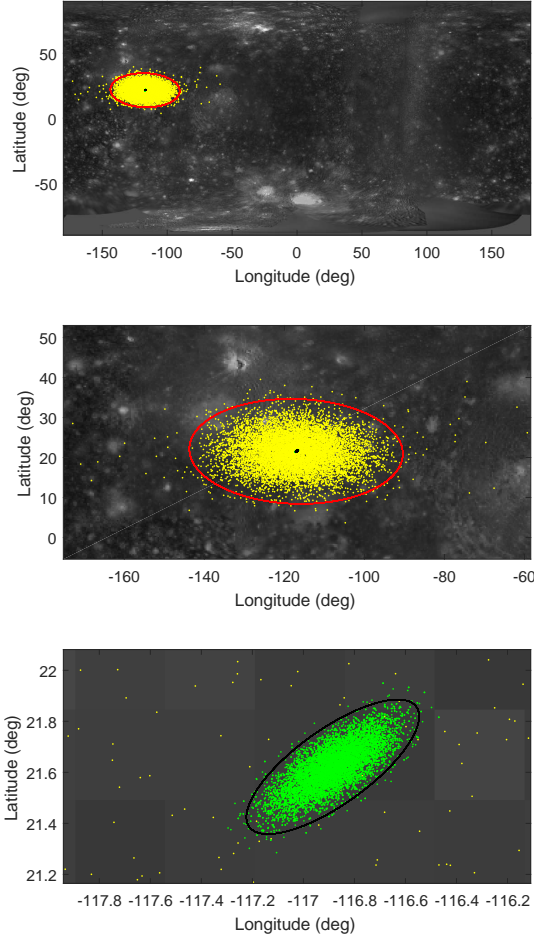


Figure 7. Outcome of the disposal event on Callisto. Each yellow dot represent a single iteration of the Monte Carlo analysis for Case I. The green dots, in a much smaller ellipse, are the results of Case II.

Figure 7 shows the results of the disposal segment. Here, all cases resulted in an impact at the moon Callisto. The nominal targeted location was zero B-R and B-T parameters, to target the moon at bulls eye. For the B-plane of the disposal incoming trajectory mean, that translated in a latitude

of 21.6 deg and a longitude of -116.9 deg. Case II mean results are placed around those values. However, while for Case I, all the points in the simulation comply with the disposal requirement, there is a larger spread in the results, mainly caused by not having the extra TCM implemented.

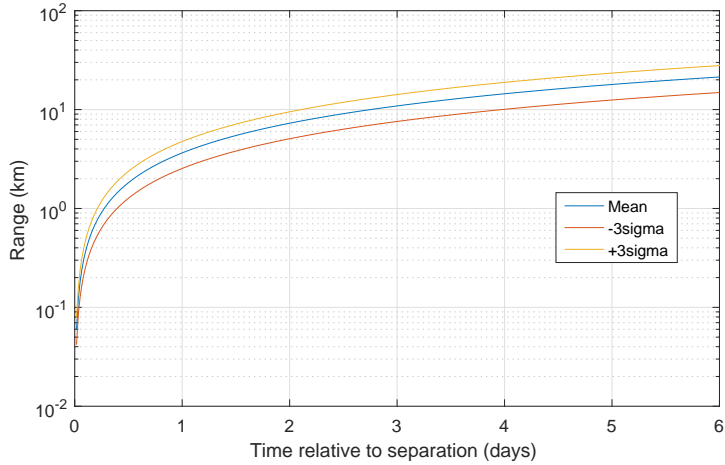


Figure 8. Average range between EMFM and ELSA and 3σ curves from deployment to first burn. The results correspond to a ten thousand cases Monte Carlo simulation.

The range results for the separation analysis between ELSA and EMFM are shown in Figure 8. The outcome of the separation analysis showed that for all the ten thousand iterations of the Monte Carlo simulation, ELSA and EMFM maintain a safe range distance between each other before the application of the first maneuver. Therefore, the possibility of recontact during this phase is negligible.

The Monte Carlo analysis validated the nominal trajectory design and increased the confidence on the feasibility of the mission. This analysis also allowed a preliminary assessment of the statistical ΔV budget at an early stage in the design process. For the two particular set of assumptions, the results show that the mission can be accomplished with a satisfactory level of confidence by implementing the correct number of TCMs.

APPLICATION TO OTHER MISSIONS

The trajectory design can be applied to small spacecraft that would be carried as a secondary payload in future interplanetary missions. The trajectory design that was introduced in this paper is dependent on two consecutive flybys in two distinct celestial bodies, where the second one has lower planetary protection requirements, to enable a direct disposal. Other potential concepts may consider consecutive encounters between a single celestial body with no strict planetary protection regulations. Pi-transfers represent an appropriate opportunity to release the secondary probe in these circumstances. Another alternative is a probe that is decommissioned in deep space after its first flyby. To illustrate the applications of the trajectory design, we take two examples of flown multi-flyby missions such as Galileo and Cassini. We perform a survey to find a suitable geometry that addresses the disposal strategy in a short time frame.

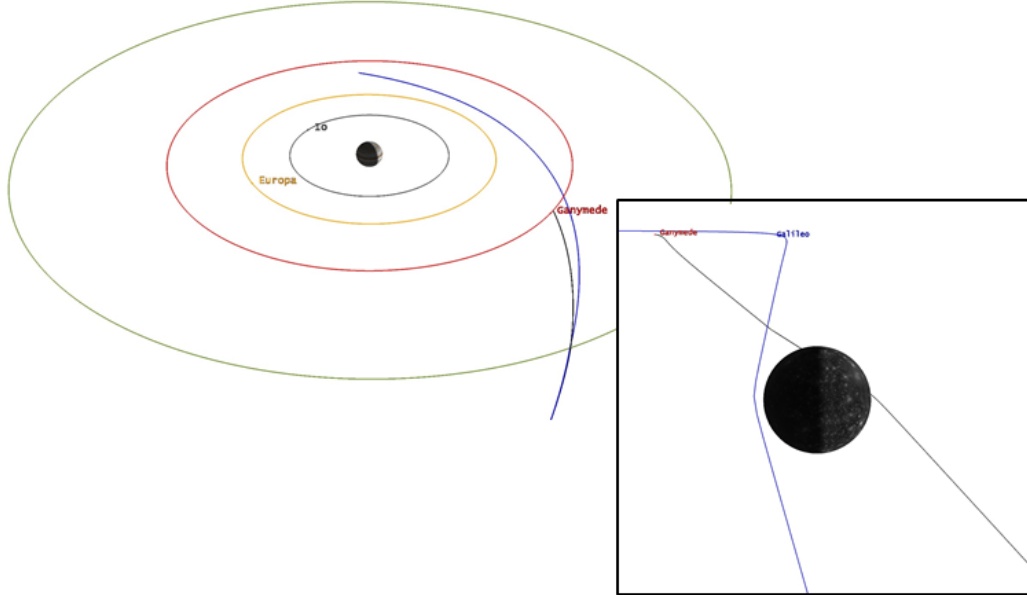


Figure 9. Captures of the nominal trajectory of a theoretical small probe attached to the Galileo spacecraft. The left picture shows the flyby approach to Callisto, where the data is gathered. Right picture shows a more detailed view of the flyby approach and the disposal in Ganymede. The blue line represents the nominal Galileo trajectory while the black line is the theoretical secondary spacecraft trajectory.

Galileo mission

In this case study, we identified potential opportunities where the primary mission performs a pi-transfer or two consecutive flybys in a short time span. In this example, Callisto flyby number 9 was chosen⁶ to design a mission that would produce a plume in this moon and that would impact in Ganymede right after. Figure 9 shows a capture of the nominal trajectory at the moment of the first flyby. Since the nominal trajectory of the primary mission plans a high altitude flyby, the probe has to modify its B-plane targeting to release the KI and pass through the generated plume. As a consequence, the outbound trajectory is severely affected by the post-flyby conditions. Hence, in this case, it is more advantageous to select an opposite B-plane aimpoint with respect to the primary mission, in order to minimize propellant consumption for the disposal maneuver afterwards. The mission ends with an impact in Ganymede, approximately one day after the flyby in Callisto.

Cassini mission

The same approach was applied to the Cassini mission. An opportunity was found in flyby number 35 at Titan, T35, followed by a flyby at Iapetus, I1, after 11 days.¹¹ This time, the trajectory design could be implemented in different concept since the atmosphere of Titan would be too dense to allow particles to be captured by the probe. However, valuable data could be gathered by flying through the atmosphere at low altitudes. In this example, a probe without an impactor is deployed from the Cassini spacecraft to perform a flyby as low as 100 km to posteriorly dispose in Iapetus by a direct impact. This mission requires a higher ΔV but it could be used for instance as a test for a heatshield.

FUTURE WORK

Future efforts include the application of this concept to other planned interplanetary missions. Potential multi-flyby concepts in planetary systems such as Saturn may benefit from the addition of an inexpensive secondary spacecraft to augment the science return with no risk to the primary. From an academic perspective, the study of this concept applied to heritage missions provides value to estimate the opportunity space available to implement added secondary missions.

Improved estimates of navigation, pointing and thruster performance would improve simulation fidelity. In this paper, both conservative and optimistic estimates were made based on prior missions. A more detailed analysis, including simulation of TRN, AutoNav software performance, and propulsion system testing results, should be implemented in future efforts. Alternatively, the trajectory validation method may be utilized to estimate the orbital determination and propulsion performance requirements for a particular mission to be performed. At an early stage of the trajectory design process, the validation technique would be able to quantify the feasibility of a mission by running the statistical analysis associated with a nominal point trajectory.

CONCLUSION

A trajectory design and validation method for an impactor mission concept to create artificial plumes was presented in this paper. A case study based on a single-string spacecraft with a kinetic impactor on board that deploys from the Europa Multi-Flyby Mission was selected to illustrate the design. The nominal solution consisted of four critical events that addressed the plume generation, the avoidance of Europa, and the final decommissioning phase. To validate this trajectory, a Monte Carlo simulation was used to evaluate navigational and maneuver performance errors. A total of ten thousand iterations for two separate set of assumptions were performed using this method. The results produced data to quantify the magnitude of the required TCMs to accomplish the mission with a satisfactory level of confidence. Mission requirements were met for the two cases with different fidelity. The trajectory design approach presented in this paper was applied to heritage missions to illustrate the potential application to future interplanetary secondary spacecraft.

ACKNOWLEDGMENTS

The authors of this paper would like to thank the NASA Ames Research Center management for their support and guidance. We greatly appreciate the NASA Ames Space Science and Astrobiology Division, in particular Dr. Anthony Colaprete, and Dr. Chris McKay for their invaluable inputs. Finally, a special recognition to the NASA Ames Mission Design Division team for their fundamental contribution in the development of this project, in particular Scott Richey, Dr. Antonio Ricco, and Anthony Genova.

REFERENCES

- [1] Lam, T., Arrieta-Camacho, J.J., and Buffington, B., *The Europa Mission: Multiple Europa Flyby Trajectory Design Trades and Challenges*, AAS 15-67, Vail, Colorado, August 9-13, 2015.
- [2] Martin-Mur, T.J., Ionasescu, R., Valerino, P., Criddle, K., and Roncoli, R., *Navigational Challenges For a Europa Flyby Mission*, 24th International Symposium on Space Flight Dynamics, Laurel, Maryland, May 5-9, 2014.
- [3] Valerino, P.N., Buffington, B., Criddle, K., Hahn, Y., Ionasescu, R., Kangas, J., Martin- Mur, T.J., Roncoli, R., and Sims, J., *Preliminary Maneuver Analysis For The Europa Clipper Multiple-Flyby Mission*, AIAA/AAS Astrodynamics Specialist Conference, AIAA SPACE Forum, (AIAA 2014-4461), San Diego, California, 4-7 August, 2014.
- [4] Buffington, B., *Trajectory Design For The Europa Clipper Mission Concept*, AIAA/ AAS Astrodynamics Specialist Conference, AIAA SPACE Forum, (AIAA 2014-4105), San Diego, California, 4-7 August, 2014.
- [5] Uphoff, C., Roberts P. H., and Friedman L. D., *Orbit Design Concepts for Jupiter Orbiter Missions*, Paper AIAA-74781, presented at AAS/AIAA Astrodynamics Conference, Provincetown, MA., USA, 1979.
- [6] Meltzer M., *Mission to Jupiter: a History of the Galileo Project* , NASA SP 2007 4231, p. 203-281.
- [7] Taylor, C.J., and Kiregman D. J., *Minimization on the Lie Group SO(3) and Related Manifolds* , Technical Report No. 9405. Yale University, April, 1994.
- [8] Bhaskaran S. *Autonomous Navigation for Deep Space Missions* , SpaceOps 2012 Conference, Stockholm, Sweden, June, 2012.
- [9] Roth L., Saur J., Rutherford K.D., Strobel D.F., Feldman P.D., McGrath M.A., and Nimmo F., *Transient Water Vapor at Europas South Pole*, Science 10 Jan 2014, Vol. 343, Issue 6167, pp. 171-174.
- [10] Vaquero M., Hahn Y., Stumpf P., Valerino P., Wagner S., and Wong M., *Cassini Maneuver Experience for the Fourth Year of the Solstice Mission*, AIAA/AAS Astrodynamics Specialist Conference (AIAA 2014-4348) , AIAA SPACE Forum, San Diego, California, 4-7 August, 2014.
- [11] Roth D., V., Bordi J., Goodson T., Hahn Y., Ionasescu R., Jones J., Owen W., Pojman J., Ian Roundhill I., Santos S., Strange N., Wagner S., Wong M., *Cassini Tour Navigation Strategy*, Proceedings of the 16th International Technical Meeting of the Satellite Division of The Institute of Navigation (ION GPS/GNSS 2003) September 9 - 12, 2003, Portland, OR.